

This article was downloaded by:  
On: 25 January 2011  
Access details: Access Details: Free Access  
Publisher *Taylor & Francis*  
Informa Ltd Registered in England and Wales Registered Number: 1072954 Registered office: Mortimer House, 37-41 Mortimer Street, London W1T 3JH, UK



## Separation Science and Technology

Publication details, including instructions for authors and subscription information:  
<http://www.informaworld.com/smpp/title~content=t713708471>

### Criteria for Selection of an Adsorbent for a Temperature Swing Process: Applied to Purification of an Aliphatic Solvent Contaminated with Aromatic Solutes

Michael J. Matz<sup>a</sup>; Kent S. Knaebel<sup>a</sup>

<sup>a</sup> DEPARTMENT OF CHEMICAL ENGINEERING, THE OHIO STATE UNIVERSITY, COLUMBUS,  
OHIO

**To cite this Article** Matz, Michael J. and Knaebel, Kent S.(1990) 'Criteria for Selection of an Adsorbent for a Temperature Swing Process: Applied to Purification of an Aliphatic Solvent Contaminated with Aromatic Solutes', *Separation Science and Technology*, 25: 9, 961 — 984

**To link to this Article:** DOI: 10.1080/01496399008050378

URL: <http://dx.doi.org/10.1080/01496399008050378>

## PLEASE SCROLL DOWN FOR ARTICLE

Full terms and conditions of use: <http://www.informaworld.com/terms-and-conditions-of-access.pdf>

This article may be used for research, teaching and private study purposes. Any substantial or systematic reproduction, re-distribution, re-selling, loan or sub-licensing, systematic supply or distribution in any form to anyone is expressly forbidden.

The publisher does not give any warranty express or implied or make any representation that the contents will be complete or accurate or up to date. The accuracy of any instructions, formulae and drug doses should be independently verified with primary sources. The publisher shall not be liable for any loss, actions, claims, proceedings, demand or costs or damages whatsoever or howsoever caused arising directly or indirectly in connection with or arising out of the use of this material.

## **Criteria for Selection of an Adsorbent for a Temperature Swing Process: Applied to Purification of an Aliphatic Solvent Contaminated with Aromatic Solutes**

**MICHAEL J. MATZ and KENT S. KNAEBEL\***

DEPARTMENT OF CHEMICAL ENGINEERING  
THE OHIO STATE UNIVERSITY  
COLUMBUS, OHIO 43210

### **Abstract**

Temperature swing adsorption (TSA) is different in several respects from conventional adsorption. This paper explores the distinctions from the standpoint of adsorbent characteristics. In particular, a fixed-bed TSA process is considered for separating dilute aromatics from aliphatics (e.g., toluene and/or xylene in heptane). Relevant adsorbent characteristics include thermal-exchange capacity and properties that affect dissipative effects, e.g., intraparticle diffusivity, bed permeability, axial dispersion coefficient, and thermal diffusivity. Many of the dissipative effects can be manipulated by adjusting particle size, though trade-offs exist that have no clear-cut technical resolution. The adsorbents considered were silica gel, activated alumina, activated carbon, zeolite 13X, and a polymeric adsorbent (XAD-7). Silica gel was selected due to its superior thermal-exchange capacity. The other properties did not vary enough among the other adsorbents to compensate for their lesser capacities.

### **I. INTRODUCTION**

The intent of this paper is to explain criteria for screening potential adsorbents for a temperature swing adsorption (TSA) application. The criteria for a TSA process are different than for conventional adsorption in that more properties are relevant, e.g., those that affect thermal response. Furthermore, some intuitively obvious criteria applied for ordinary adsorption are invalid for TSA, such as maximizing the uptake capacity. Following a brief review of the origins of TSA, the adsorbent selection criteria will be cited and then explained in detail.

The original TSA processes were developed to reduce the negative im-

\*To whom correspondence should be addressed.

pact of conventional adsorption and ion-exchange processes, primarily associated with regeneration. Wilhelm conceived of parametric pumping (PP) during the early 1960s. Cycling zone adsorption (CZA) was proposed shortly thereafter by Pigford and coworkers. These were the basis of dozens of subsequent studies that have been reviewed by Sweed (1) and Wankat (2).

The basic idea for both PP and CZA was to pump fluid through a fixed bed of adsorbent while imposing synchronous temperature shifts; the result was an effluent having oscillating concentration. Thus, the adsorbent could be partially regenerated in place by using low-grade heat and *no* foreign regenerant. PP involves cyclic variations of temperature and flow direction; CZA employs only temperature oscillations.

A modification of CZA, called recycled temperature swing adsorption (RTSA), involves recycle of the solute-rich and/or solute-lean portions of the product, one version of which was suggested by Rieke (3), and another was studied by Kayser and Knaebel (4).

Several potential applications of liquid-phase TSA exist in diverse fields, including petroleum processing and water purification. Dilute solutes present at low concentrations in solvents are commonly difficult to remove by conventional separation processes, resulting in high capital or operating costs. In contrast, conventional adsorptive separations typically are effective at purifying solvents, but require a separate regenerant, and so they are expensive and inconvenient to employ for cyclic use.

Heat transfer is vital in TSA processes because performance is governed by temperature waves that propagate through the fixed bed of adsorbent. These waves have a specific velocity which is a function of the fluid velocity, heat capacities, and other variables as given by Knaebel and Pigford (5). Rapid conduction within the adsorbent particles allows ideal response to temperature. Conversely, slow conduction, significant axial conduction, or heat loss through the column wall leads to degradation of the thermal wave, and corresponding dampening of the concentration shifts.

A primary goal of TSA processes is to achieve sharp concentration and thermal fronts, e.g., through the reduction of particle size. The net result of such sharp fronts is increased productivity due to decreased recycle during the regeneration step. An approach of this sort has been termed "intensification" by Wankat (2) for gas-phase adsorption processes. Inherently, intensification implies that better productivity can be achieved for short and fat (versus long and thin) beds, with the same pressure drop.

The adsorbent characteristics of interest for TSA include equilibrium adsorption capacity and its temperature sensitivity, particle size and shape, intraparticle diffusivities and conductivities, and chemical and physical characteristics of the solid. These, in turn, affect rates of adsorption, de-

sorption, and conduction, the necessary size of the adsorbent bed, pressure drop, and overall separation performance.

## II. GENERALIZATIONS ON ADSORBENT PROPERTIES

When equilibrium between fluid and solid occurs readily, the recycled temperature swing adsorption (RTSA) process can be accurately simulated by a relatively simple equilibrium model. Furthermore, separation performance is easily maximized if mass transfer resistances are negligible. In that case it is easy to isolate products of distinct concentrations (because there is less rounding associated with mass transfer zones, and consequently less product having intermediate concentration), and it is simpler to grasp the effects of temperature, step times, and flow rate, which are left as the primary independent variables. Many of those topics will be discussed more fully in a subsequent paper on RTSA process performance (6).

The implication is that it is essential to understand the nature of the adsorption equilibria that drive the process, as well as the dissipative effects that constrain its performance. Unfortunately, the fundamental properties that can be manipulated to reduce one dissipative effect often, in so doing, increase another.

### A. Equilibrium Adsorption Isotherms

Unlike conventional adsorption processes for which high equilibrium capacity is always beneficial, isotherm shape is more critical to TSA processes. In RTSA cycles especially, higher "favorableness" (i.e., concavity downward) decreases the separability with increasing feed concentration. In fact, a rectangular isotherm would preclude purification of a solvent by TSA. Kayser and Knaebel (4) mention that even for systems that exhibit Freundlich isotherms, isolation of a pure solvent is impossible because the slope of the Henry's law region of the high temperature isotherm is, by definition, very large and insensitive to temperature.

The reason for this unusual behavior of RTSA processes is that the maximum feed concentration (for which recovery of the pure solvent is possible) is determined by the intersection of the Henry's law extrapolation of the high temperature isotherm with the low temperature isotherm, as shown in Fig. 1 for the case of toluene dissolved in heptane with silica gel as the adsorbent. As a result, better process performance can be achieved with a dilute feed and by selecting an adsorbent that exhibits linear isotherm behavior or by ensuring that the temperature swing is sufficiently large to achieve adequate divergence of the isotherms.

In multicomponent adsorption, isotherm shape can be affected by other solutes. As the concentration of a particular solute increases, the isotherm

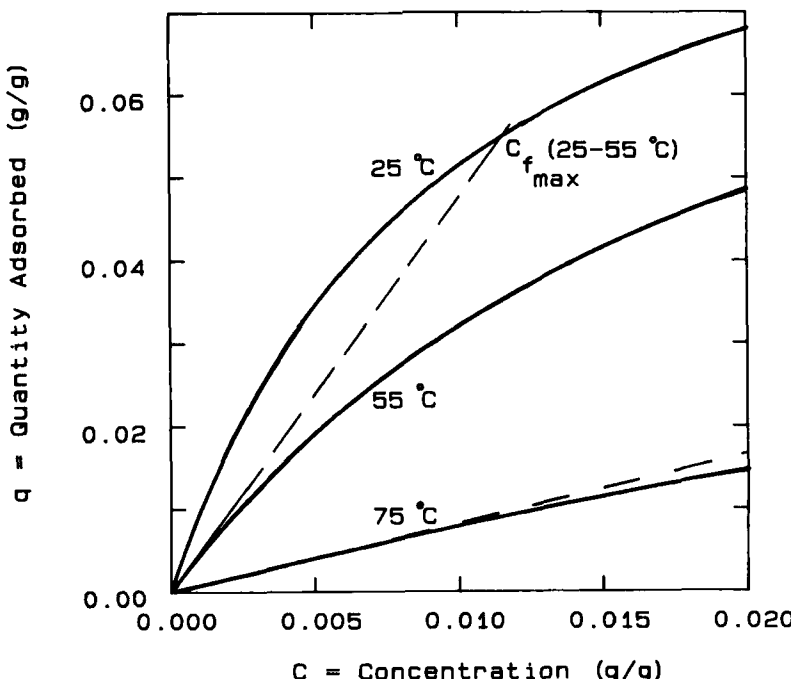


FIG. 1. Isotherms of toluene (in *n*-heptane) on silica gel, illustrating the interaction that determines the maximum feed concentration. Note that  $c_{f_{\max}} (25-75^{\circ}\text{C}) \approx 0.1 \text{ g/g}$ , but the value is uncertain due to extrapolation.

slope for any less strongly adsorbed component decreases. Consequently, the separation factor (which is the ratio of Henry's law coefficient of the solute to that of the most strongly adsorbed component) decreases, and separation performance diminishes. The reverse is true, however, for concentrating more strongly adsorbed species.

### B. Rates of Adsorption and Desorption

Within a packed bed, mass transfer effects include film diffusion, axial dispersion, and intraparticle diffusion. These are influenced by geometry, including bed diameter and particle size, and by operating conditions, such as interstitial flow rate and temperature.

The film mass transfer coefficient,  $k_c$ , can be determined from an empirical correlation, e.g., as suggested by Wilson and Geankoplis (7) for  $Re = 0.002$  to 1500. The dependence of  $k_c$  (at 25°C) on superficial velocity and particle size is shown in Fig. 2, in which heptane and toluene are taken

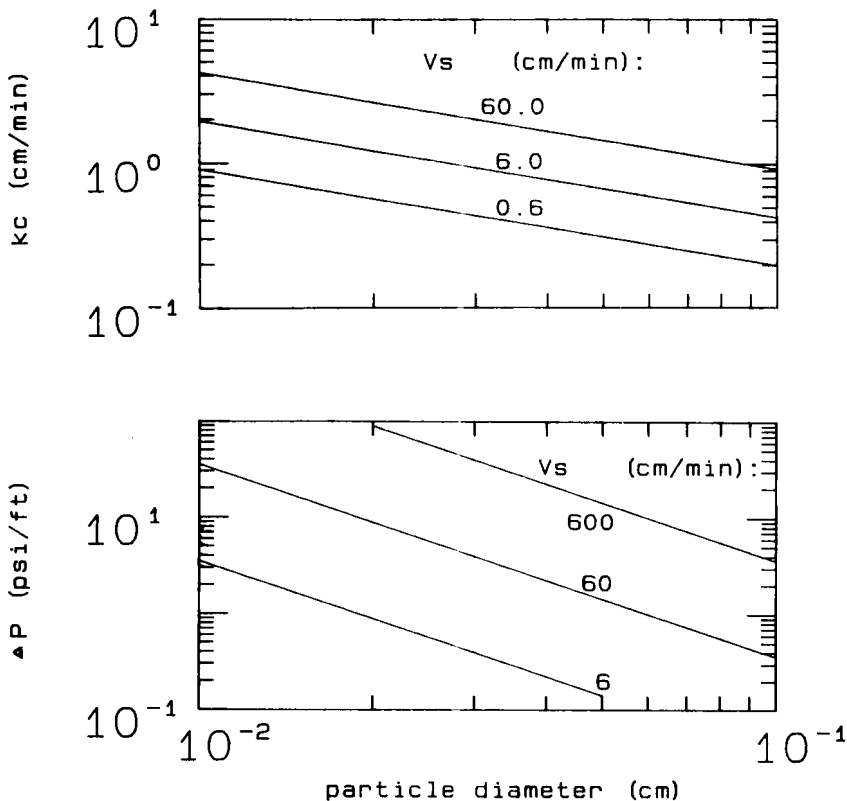


FIG. 2. (Top) Packed bed mass transfer coefficients and (bottom) pressure drop per length values for the toluene-heptane system using a silica gel adsorption column.

to be the solvent and solute, respectively. As flow rate increases, the mass transfer coefficient increases and intraparticle diffusion becomes the dominant mass transfer resistance.

Axial dispersion adversely affects concentration fronts and is affected by velocity and particle size. The Peclet number,  $Pe = vd_p/D_Z$ , which governs axial dispersion, for liquids is basically constant (i.e.,  $Pe = 0.45$ ) for  $Re = 0.01$  to 10 as given by Sherwood et al. (8). Thus, although the dispersion coefficient increases with velocity, the sharpness of concentration profiles is virtually unaffected by velocity. The particle size effect on dispersion is governed by the Reynolds number and by the observed additional effect of nonuniform packing near the column wall for relatively large particles, i.e., for  $d_c < 25d_p$ .

It is also important that the solute exhibit a large intraparticle diffusivity, but this property can depend on the pore size distribution as well as the internal mechanism of diffusion. Values generally increase as pore diameter increases, but other factors including temperature, particle diameter, type of adsorbent, and solute concentration affect it.

Similarly, it is important that the thermal wave be a nearly perfect step-function. This enables a sharp composition front to form and propagate through the bed. In order to achieve a square wave, the column must have minimal dead-volume, and the thermal diffusivity of the adsorbent must be large, yet axial conduction must be minimized.

### C. Pressure Drop

As stated above, reducing particle size can allow local equilibrium to be achieved. Consequently, the process is simpler to operate and to understand from a theoretical viewpoint. Unfortunately, reducing particle size leads to dramatically larger pressure drop.

Pressure drop for packed beds can be estimated via the Blake-Kozeny equation, which applies for  $Re < 10 (1 - \epsilon)$ :

$$\Delta P/L = 150 \frac{\mu v (1 - \epsilon)^2}{d_p^2 \epsilon^3} \quad (1)$$

Figure 2 shows the effect of particle diameter and superficial velocity on pressure drop. Industrial columns are typically short and fat (e.g.,  $L/d_c \approx 2$ ) in order to reduce pressure drop, but they also exhibit nearly adiabatic behavior, which is important to TSA processes. Longer and thinner columns suffer from increased pressure drop but reduced dead-volume, resulting in sharper concentration fronts and improved process performance.

### D. Chemical and Physical Characteristics

Aside from adsorption and rate properties, certain adsorbents can possess undesirable characteristics for application to RTSA. Attrition due to adsorptive fracture, for example, has been observed for silica gel. In addition, in the present application chromatographic-grade alumina appears to be fused together, which leads to diminished interstitial void space. Certain types of adsorbents are available in only a few, fairly large particle sizes, such as those made by emulsion polymerization. Adsorbents with low density, e.g., activated carbon, which has a large adsorption capacity (on a per unit mass basis), require larger column volumes to achieve similar productivities.

### III. SPECIFIC ADSORBENTS FOR REMOVING AROMATICS FROM ALIPHATIC SOLVENTS

This section presents results obtained from equilibrium studies and evaluation of adsorbent properties, in particular for separating dilute aromatic solute(s) from an aliphatic solvent. Several common adsorbents were studied including silica gel (Davison Grade 12 [ $28 \times 200$  mesh] and Grade 408 [ $12 \times 28$  mesh]), activated alumina (Alcoa Grade CG20 [ $140$  mesh]), activated carbon (Calgon type CAL [ $12 \times 40$  mesh]), zeolite Molecular Sieve 13X (Union Carbide [ $16 \times 40$  mesh]), and XAD-7 acrylic ester resin beads (Rohm and Haas [ $40 \times 50$  mesh]). The solvent was *n*-heptane, and both toluene and xylene were investigated as solutes (all liquids were Fisher HPLC grade). Temperatures of 0, 30, 55, and 80°C were studied.

#### A. Experimental Methods and Analysis

Fresh activated carbon was used without any initial regeneration. The remaining adsorbents were regenerated by the following procedures before performing equilibrium experiments. Silica gel (Grade 12) and alumina were heated under vacuum at 200°C for 8 h or more, and Molecular Sieve 13X was vacuum regenerated at 400°C. XAD-7 resin was washed with isopropyl alcohol, soaked in distilled water, and dried at 60°C.

Standard solutions were made by adding a known amount of solute, either toluene or xylene, to a certain amount of heptane. These concentrations were correlated to UV-absorbance so that unknown samples could be evaluated. Solution-to-adsorbent mass ratios of 3 to 18 were used; the value was increased as temperature decreased, between 80 and 0°C.

To obtain each isotherm, a preweighed sample of adsorbent was placed in a 40-mL vial. Each vial was sealed with a Teflon cap that had an integral valve that allowed a liquid sample to be withdrawn by a syringe. Each vial was filled with solution having an initial concentration of 0.0001 to 0.02 g(solute)/g(solution) (100 to 20,000 ppm) and was then placed in a constant temperature bath. Equilibration occurred for approximately 24 h, then samples were drawn, and final concentrations were measured via a Hewlett-Packard 8452 ultraviolet spectrophotometer. In this manner, capacity data at temperatures of 0, 30, 55, and 80°C were obtained.

Following equilibration, the amount adsorbed was determined from a simple material balance. In most cases it was appropriate to ignore solvent uptake since it was present in great excess. The polymeric resin, however, swelled to a significant extent in transforming from the dry to the normal working state. As a result, the solvent required for swelling was taken into account separately.

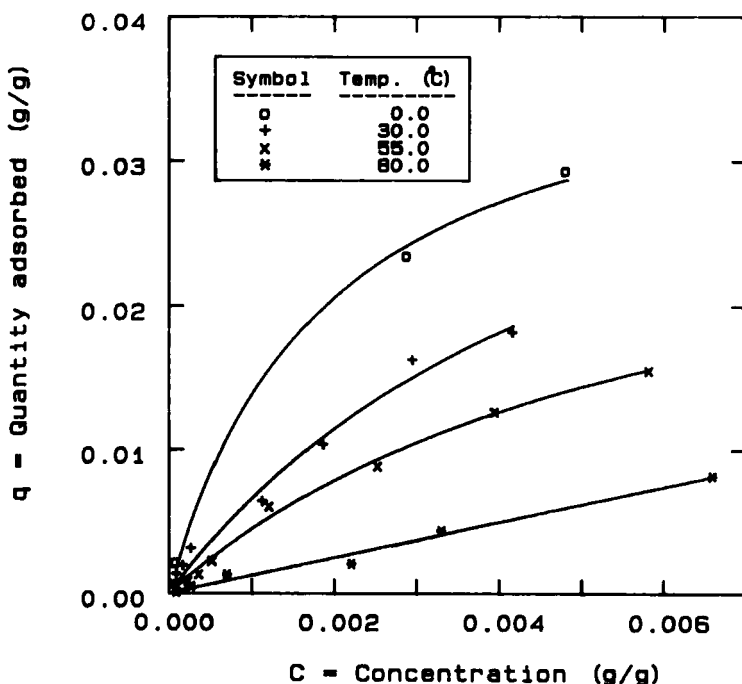
### B. Equilibrium Isotherms

The adsorption isotherms of toluene and xylene on silica gel are shown in Figs. 3 and 4. The data were fit with Langmuir isotherm parameters

$$q_i^* = \frac{A_i(T)c_i}{1 + B_i(T)c_i} \quad (2)$$

for each temperature investigated, as shown in Table 1. In this study, final equilibrium concentrations were less than 0.01 g(solute)/g(solution). Despite that, it appears reasonable to apply the isotherm data to higher concentrations because the data are relatively smooth and because it is primarily the Henry's law region of the isotherm that is critical for assessing RTSA performance.

Further experiments with silica gel studied single-solute isotherms in the context of dilute mixtures, primarily to discern whether competition affected the isotherms relative to their pure component behavior. In order



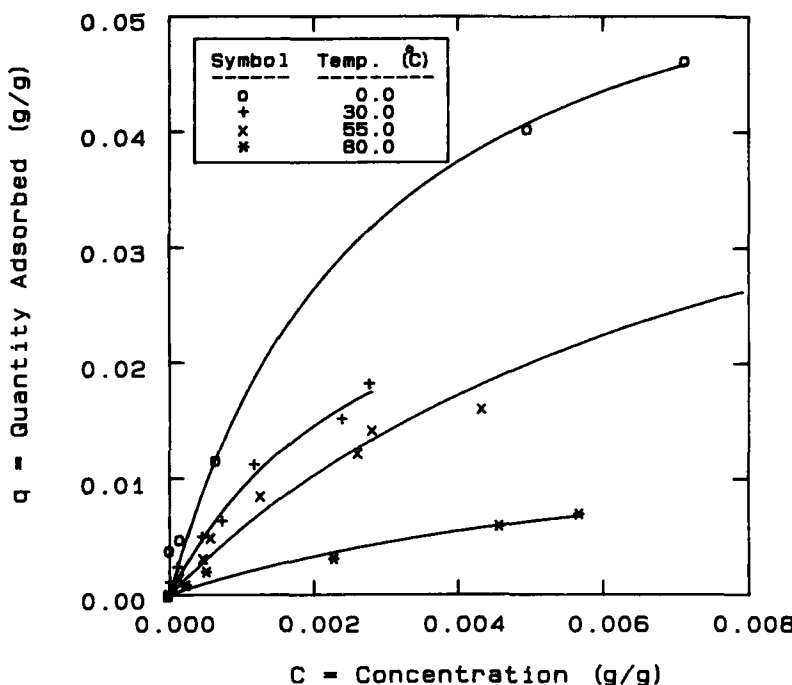


FIG. 4. Xylene adsorption isotherms with *n*-heptane as the solvent on silica gel at 0, 30, 55, and 80°C.

TABLE 1  
Langmuir Isotherm Parameters for Xylene (1) and Toluene (2) on Silica Gel<sup>a</sup>

Parameter	Temperature (°C)			
	0	30	55	80
<i>A</i> <sub>1</sub>	22.36	12.03	6.28	2.01
<i>A</i> <sub>2</sub>	17.46	7.77	5.16	1.23
<i>B</i> <sub>1</sub>	348.0	327.0	113.0	121.0
<i>B</i> <sub>2</sub>	390.0	177.0	159.0	0.0

$\ln A_1 = -38.30 + 22245.6/T - 2988230/T^2$   
 $\ln A_2 = -42.44 + 24421.7/T - 3297912/T^2$   
 $B_1 = A_1 \times 20.3$   
 $B_2 = A_2 \times 23.1$

<sup>a</sup>The maximum concentration was about 1% (0.01 g(solute)/g(solution)).

to extract mixture composition data, the UV spectra had to be deconvoluted. The pure component absorbances were shown to combine linearly when observed in mixtures, and unknown sample concentrations of both toluene and xylene could be easily determined.

Figure 5 shows the equilibrium uptake of toluene, accounting for the adsorption of xylene which was initially present at 700 ppm. The data fall essentially along the pure component isotherm, indicating negligible competition among solutes and implying that a simple, multicomponent equilibrium theory may be appropriate in the experimental range studied. Incidentally, the pure component xylene isotherm was also duplicated in the presence of toluene.

Figures 6 and 7 show the equilibrium isotherms of toluene on alumina and activated carbon. Both adsorbents display temperature sensitivity at relatively high concentrations, but the Henry's law region isotherm slopes at different temperatures approach a constant value. In particular, alumina

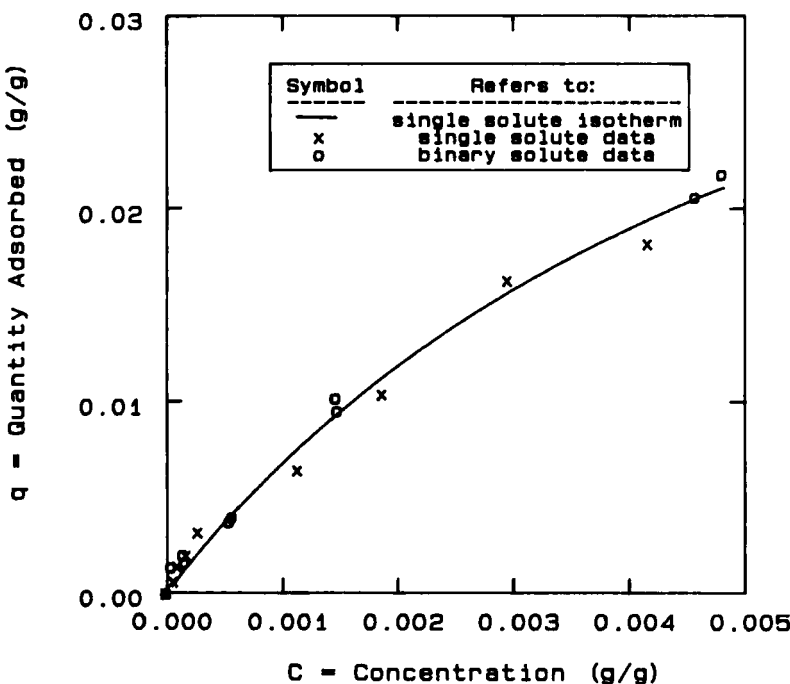


FIG. 5. Toluene adsorption from xylene-containing heptane solvent on silical gel at 30°C compared with single solute data.

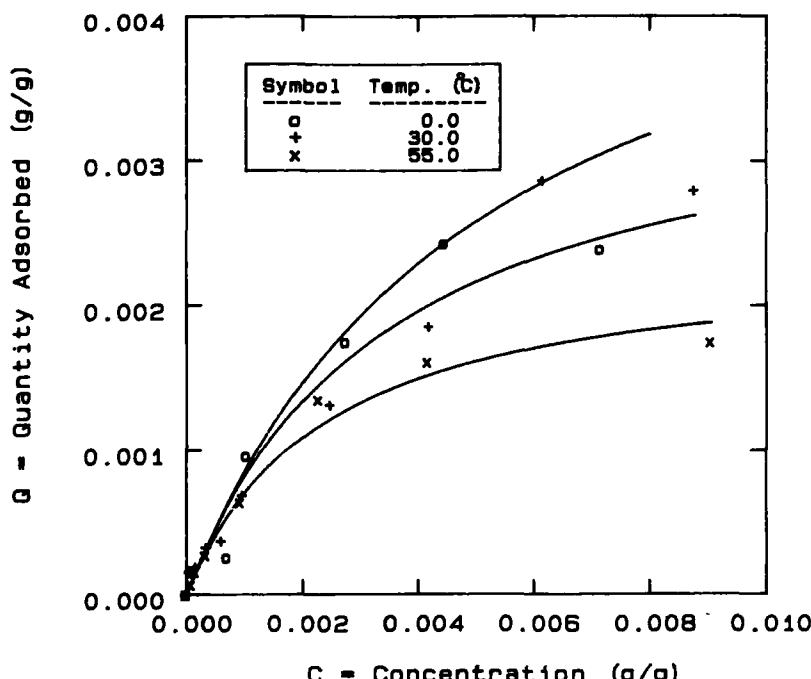


FIG. 6. Toluene adsorption isotherms with *n*-heptane as the solvent on activated alumina at 0, 30, and 55°C.

isotherms at 0, 30, and 55°C are virtually the same below 0.001 g(solute)/g(solution) (1000 ppm), and carbon data show similar behavior below 0.001 g(solute)/g(solution) (1000 ppm). Activated alumina isotherms follow the Langmuir form and are about one-third the capacity of silica gel. Activated carbon exhibits Freundlich-type isotherms and has a capacity similar to silica gel. Neither alumina nor carbon, however, is appropriate for purification of aromatic-containing aliphatic solvents via RTSA because of their Henry's law region isotherm behavior.

Finally, Molecular Sieve 13X and polymeric resin XAD-7 were determined to have negligible temperature sensitivity as shown in Fig. 8. The equilibrium capacity of toluene for 13X is about 5 times that of silica gel, but it does not vary appreciably with temperature. Likewise, XAD-7 is not applicable to TSA for this hydrocarbon system, although it displays a strong affinity for the aromatic solute. The amount of solvent taken up and the corresponding volume change observed in transforming from the

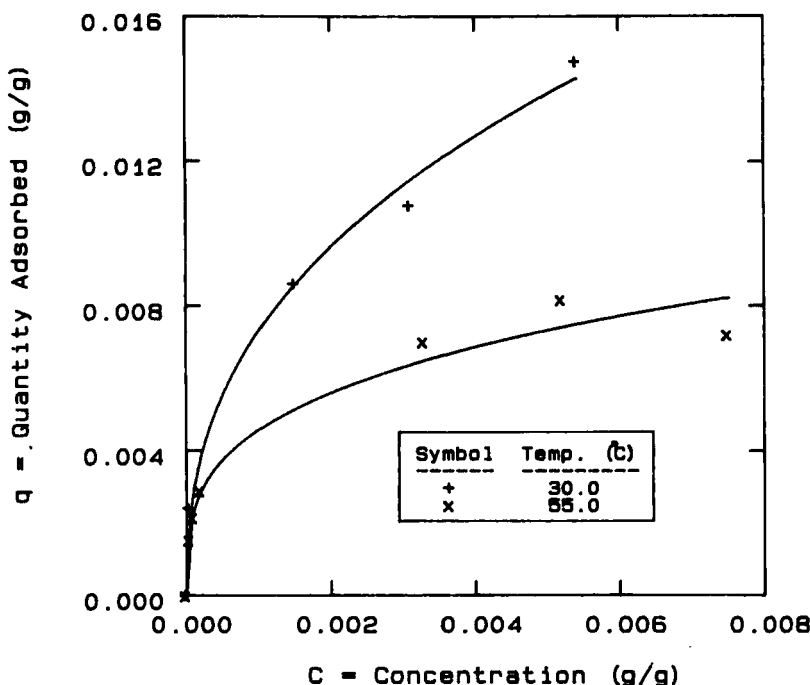


FIG. 7. Toluene adsorption isotherms with *n*-heptane as the solvent on activated carbon at 30 and 55°C. Data were collected by Barry (9).

dry to the resin working state were 2.74 g(solvent)/g(dry resin) and 2.35 mL(wet resin)/mL(dry resin), respectively.

In view of the superiority of the equilibrium capacity, silica gel has been selected as the best adsorbent for purification of aliphatic solvents via RTSA. The other adsorbents had acceptable capacities for the aromatic solute, indicating that they might be suitable in a conventional adsorption process. They were subsequently discarded for this application, however, because they exhibited insufficient selectivity and temperature sensitivity to be commercially viable. The following section considers the additional impact of dissipative effects on the final selection of an adsorbent.

#### IV. DISSIPATIVE EFFECTS FOR SILICA GEL

It is also important to understand rates of heat and mass transfer relevant to the RTSA process, i.e., the kinetics of adsorption, as well as intraparticle conduction and axial dispersion in adsorption columns. It is important for intraparticle diffusion and conduction to be rapid and for axial dispersion

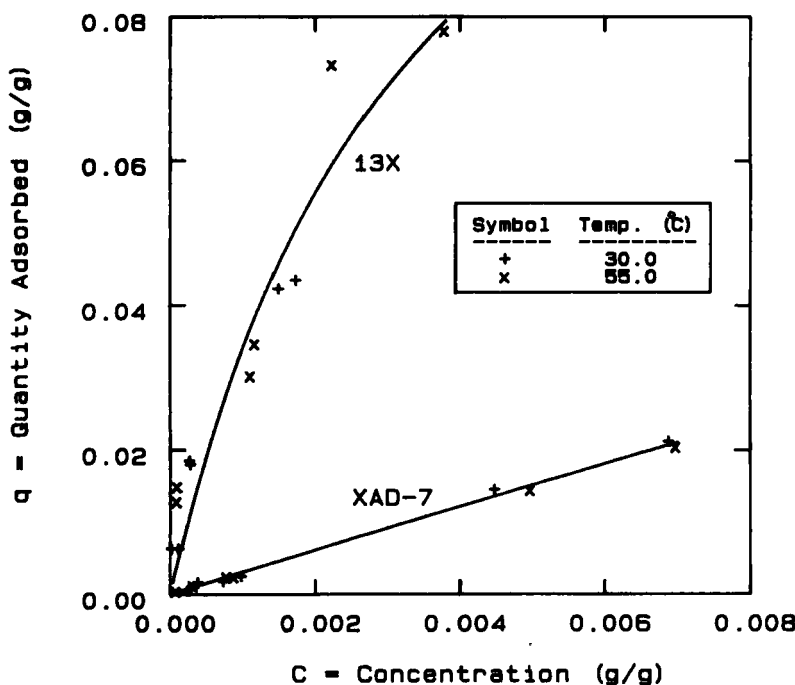


FIG. 8. Toluene adsorption isotherms with *n*-heptane as the solvent on molecular sieve 13X and XAD-7 resin at 30 and 55°C. XAD-7 data were collected by Barry (9).

and conduction to be slow. If one or more of these desirable characteristics cannot be produced, separation performance will diminish. Unfortunately, it is not possible to achieve all of these desired effects because of inherent conflicts.

#### A. Intraparticle Diffusion Rates: Experimental Methods and Analysis

Pore diffusivities have been determined using the spinning basket method. To ensure validity, the film mass transfer resistance was eliminated by performing experiments over a range of speeds to ascertain when speed no longer affected the rate of uptake. Under those conditions, pore diffusivities were calculated from concentration-time profiles.

A known mass (*M*) of regenerated silica gel was placed in the basket, and a certain volume (*V*) of *n*-heptane solvent was placed in a beaker, held at constant temperature by a water or ice bath. The basket, connected to a Dyna-Mix motor, spun at about 210 rpm, and at *t* = 0 a known amount

of toluene was injected by syringe into the solvent. Solution concentrations were measured on-line via a UV-spectrophotometer, and real-time data were stored by a microcomputer. The apparatus employed a flow-through UV quartz cell, a peristaltic pump, and minimal dead-volume to determine concentration histories. The volume of solution-to-mass of adsorbent ratio was 20 cm<sup>3</sup>/g.

The pump-around system utilized a flow rate of 30 cm<sup>3</sup>/s, which was equivalent to a 10-s dead-time and may have contributed to experimental error. Furthermore, using the flow-through cell and pump-around system, the initial concentration did not quite reach the value expected if it had been an instantaneous step change. This was compensated for by superposing the response to an imposed step change of the system in the absence of adsorbent. This yielded corrected concentration versus time profiles which were suitable for analysis.

Diffusion is presumed to be Fickian within the porous adsorbent. The transient material balance is

$$\epsilon_p D_{pore} \nabla^2 c_i = \frac{\partial}{\partial t} (\epsilon_p c_i + \rho_p q_i) \quad (3)$$

By ensuring that the composition shifts are small, it is appropriate to employ a linearization of the isotherm in order to decouple the terms within the particle. The resulting form of Fick's second law is

$$D_{eff} \nabla^2 c_i = \partial c_i / \partial t \quad (4)$$

where the effective diffusivity is

$$D_{eff} = D_{pore} \left/ \left( 1 + \frac{\rho_p \partial q_i^*}{\epsilon_p \partial c_i} \right) \right. \quad (5)$$

The solution is based on an initial condition of the adsorbent being solute-free and a boundary condition of a specified initial condition that subsequently diminishes as uptake occurs, due to the finite volume of the bath. The final result is expressed as the fraction of the ultimate uptake that has occurred at any time, and has been presented by Crank (10).

$$F = \frac{c - c_0}{c_\infty - c_0} = 1 - \sum_{i=1}^{\infty} \frac{6\beta(1 + \beta)e^{-D_{eff}p_i^2/R_p^2}}{9 + 9\beta + \beta^2 p_i^2} \quad (6)$$

where the initial and ultimate concentrations at equilibrium with the adsorbent are  $c_0$  and  $c_\infty$ , respectively.  $\beta$  is determined from material balance data and properties as

$$\beta = \rho_p V \left/ \left[ \epsilon_p M \left( 1 + \frac{\rho_p \partial q_i^*}{\epsilon_p \partial c_i} \right) \right] \right. \quad (7)$$

and  $p_i$ 's are the nonzero roots of the transcendental equation

$$\tan p_i - 3p_i / (3 + \beta p_i) = 0 \quad (8)$$

The series solution yielded the Fourier number as a function of fractional uptake, which was used to evaluate  $D_{pore}$  from the composition versus time data. Results are discussed below.

## B. Pore Diffusivity Results

In these rate studies, several particle sizes of silica gel were investigated; the average diameters were 0.0338, 0.0463, and 0.0925 cm. The smaller particles required high rotating speeds to eliminate the film resistance as compared to intraparticle resistance. This implied very small times of uptake which led to large relative error in the analysis of the concentration histories. Subsequently, the largest (0.0925 cm) silica particles were used. These particles were Davison Grade 408 which had the same physical properties of Grade 12 used in the equilibrium studies.

Figure 9 shows the concentration-time profiles for the adsorption of toluene from *n*-heptane by silica gel at 30°C. As the rotating speed was increased from 180 to 210 rpm, the concentration history was altered. This did not occur as the speed was increased to 240 rpm. Subsequently, experiments at three different temperatures were performed at both 210 and 240 rpm. Representative curves of  $D_{eff}t/R_p^2$  versus time ( $t$ ) at each temperature are shown in Fig. 10. The time of adsorption was longest at 4.5°C since capacity was greatest. Consequently, this experiment yielded the most accurate value of  $D_{pore}$ .

The calculated values of  $D_{pore}$  versus temperature are shown in Fig. 11. The results can be compared to values of ordinary diffusivity,  $D_{AB}$ , obtained experimentally or calculated via an empirical correlation (e.g., the Tyn and Calus equation), adjusted by a factor that accounts for the different environment in a particle compared to bulk solution. This factor varies between 1.30 and 1.89 for the three temperatures studied here. Since  $D_{pore}$  approaches  $D_{AB}$ , it can be concluded that the large pore-to-molecular diameter ratio for silica gel and aromatic molecules creates an excellent environment for intraparticle diffusion.

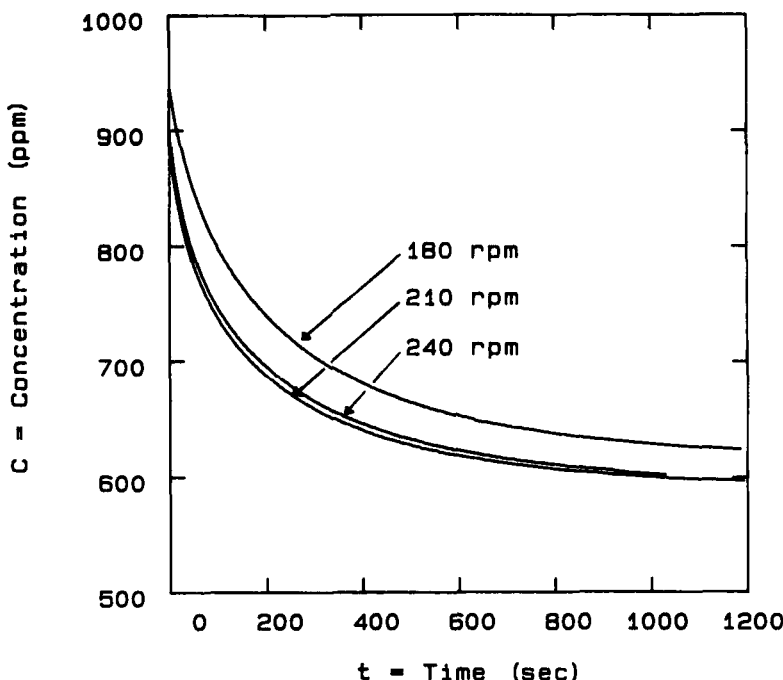


FIG. 9. Concentration-time histories obtained from spinning basket effective diffusivity experiments for toluene adsorption at 30°C on silica gel (18-20 mesh).

Temperature appears to affect this ratio and, consequently, the relationship with  $D_{AB}$ . From an RTSA viewpoint, a factor of 10 (or larger) difference in pore diffusivities as a function of temperature could result in subtle performance variations. For example, a relatively low feed temperature of, say,  $-20^{\circ}\text{C}$  may increase the deviation from local equilibrium and require more recycle and/or yield lower separation factors. This concern, however, is minimal in the range of temperatures near ambient, as shown by the data.

### C. Column Thermal Conduction: Experimental Methods and Analysis

The thermal diffusivity of the composite adsorbent and *n*-heptane solvent was determined by performing step-change experiments analogous to those for pore diffusivity, discussed in the previous section. The step change was accomplished by transferring a section of column that was loaded with

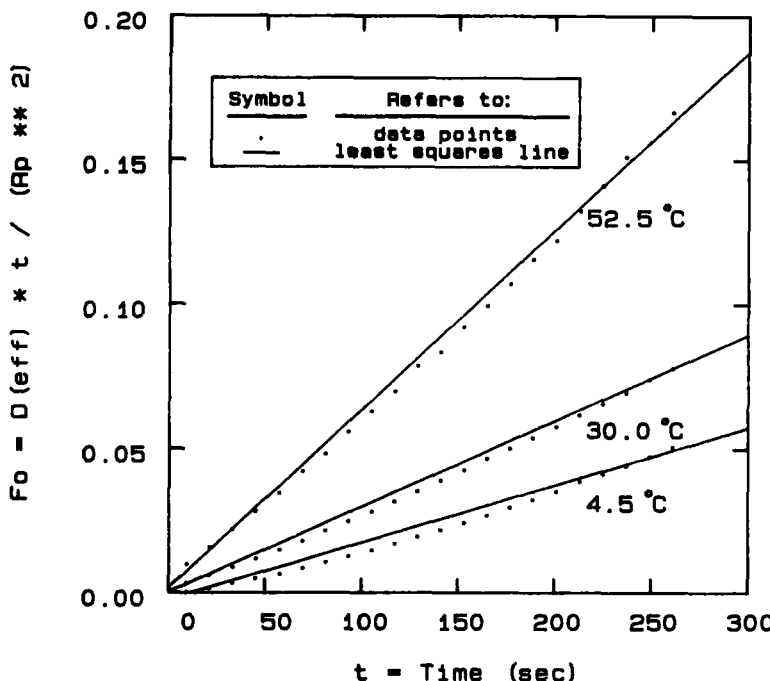


FIG. 10. Fourier number versus time for spinning basket effective diffusivity experiments investigating toluene adsorption on silica at 4.5, 30.0, and 52.5°C.

adsorbent and solvent from an ice bath to an agitated 50°C bath and recording the subsequent transient response. A thin walled stainless steel column ( $L = 22.22$  cm, o.d. = 3.80 cm, i.d. = 3.66 cm =  $2R_c$ ) was used so that the resistance to heat transfer through the wall could be neglected. End plugs made of 3 cm thick nylon were used. Thermocouples were inserted through the top end and were positioned at the center ( $r = 0$ ) and at the wall ( $r = R_c$ ).

The situation is analyzed as an infinite cylinder subjected to a step change of surface temperature. The transient energy balance is

$$\alpha_{eff} \nabla^2 T = \partial T / \partial t \quad (9)$$

The solution of this equation provided by Carslaw and Jaeger (11) is used to determine the thermal diffusivity ( $\alpha_{eff}$ ) which best fits the data. The fractional temperature change at the centerline of the cylinder is

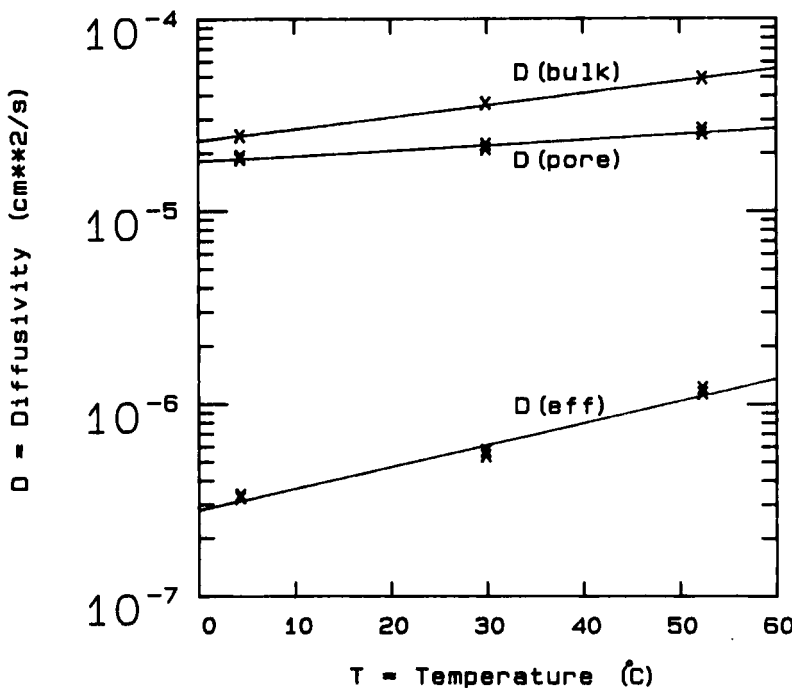


FIG. 11. Bulk, pore, and effective diffusivities for the toluene-heptane system using 18-20 mesh silica gel at 4.5, 30.0 and 52.5°C.

$$F = \frac{T - T_0}{T_\infty - T_0} = 1 - 2 \sum_{i=1}^{\infty} \frac{e^{-\alpha_{eff} s_i^2}}{s_i J_1(R_c s_i)} \quad (10)$$

where  $T_0$  and  $T_\infty$  are the initial and ultimate centerline temperatures, respectively,  $J_1$  is the Bessel function of the first kind and first order, and  $s_i$  represents one of the nonzero, real roots of the Bessel function of the first kind and zeroth order

$$J_0(R_c s_i) = 0 \quad (11)$$

In order to extract information about the solid adsorbent within the two-phase bed, the approach of Kunii and Smith (12) is taken. They investigated the heat transfer mechanism in beds of either unconsolidated particles or consolidated porous media. Adsorption columns, however, can be considered as beds of unconsolidated particles that are themselves consolidated porous media, so that both mechanisms that were originally considered by

Kunii and Smith occur within the column. In the following development the analysis is extended to apply for unconsolidated particles with an effective (combined) porosity. The effective porosity is necessary to determine the linear contributions of liquid and solid properties such as density and heat capacity. This appears justified because the intraparticle and interstitial void fractions are roughly equal.

The effective column density and heat capacity are estimated from the properties of the solid and liquid, and weighting them according to an overall void volume fraction, i.e.,  $\epsilon_p \approx \epsilon_b \approx \epsilon$ . This leads to an effective thermal conductivity,  $k_{eff}$ , which is evaluated from the experimental temperature-versus-time data. The relation proposed by Kunii and Smith can be rearranged to evaluate the unknown thermal conductivity for the solid.

$$k_s = \frac{k_f l}{\frac{1 - \epsilon}{k_{eff}/k_f - \epsilon} - \phi} \quad (12)$$

where  $l$  is a dimensionless length for heat transfer by conduction, which was determined by Kunii and Smith to be  $\approx 2/3$ , and  $\phi$  is an effective film thickness for the particles in the bed. A correlation for  $\phi$  was proposed by Kunii and Smith for gas-solid interactions. Specchia et al. (13) suggested a simpler version, viz.,  $\phi \approx 0.22\epsilon^2$ , for  $k_s/k_f > 10$ .

In order to interpret these properties as criteria for selecting an adsorbent for RTSA, the thermal diffusivity of the composite adsorbent bed and interstitial liquid is most informative. This property indicates the rapidity of response to a temperature shift, which must be high in order to maintain a sharp thermal wave. The thermal conductivity of the adsorbent is useful for comparison with published data for similar material, e.g., to validate the technique, or possibly to provide a basis for choosing among different grades of the same basic adsorbent. Since significant differences in other properties that affect thermal response (e.g., porosities, heat capacities, etc.) are common among various adsorbents, the thermal conductivity itself should not be a criterion.

#### D. Thermal Diffusion and Conduction Results

The experimental fractional temperature change at the center of the column is shown in Fig. 12 for silica gel, activated alumina, activated carbon, and glass beads, all with *n*-heptane. The data were analyzed based on radial conduction in an infinite cylinder. The glass beads (quartz) ( $d_p = 163 \mu\text{m}$ ,  $\rho_s = 2.5 \text{ g/cm}^3$ ,  $\epsilon_p = 0.0$ ,  $\epsilon_b = 0.4 = \epsilon$ ) exhibited similar behavior to activated carbon and were investigated to verify the approach

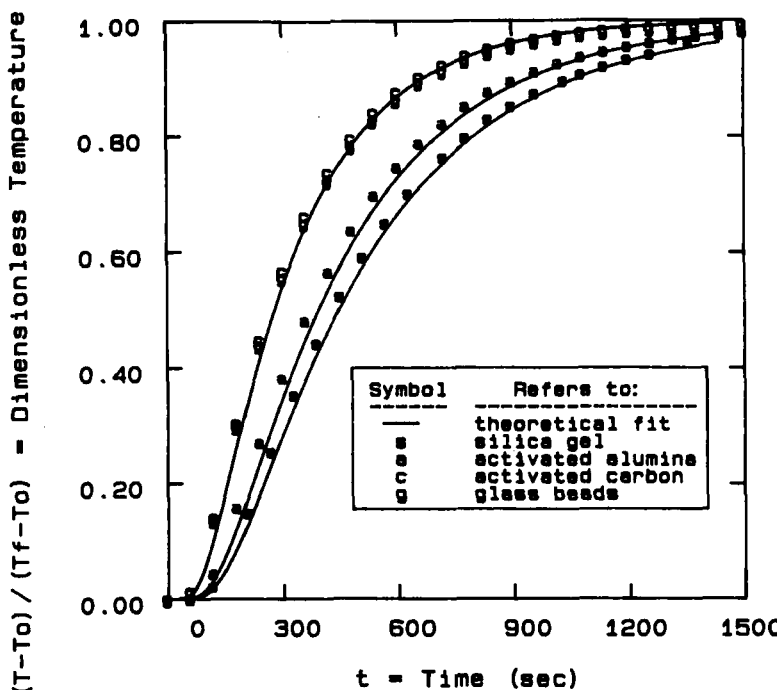


FIG. 12. Fractional temperature change versus time for silica, alumina, and carbon adsorbents with n-heptane as the solvent. Data were collected by Matz (14).

used here. Accordingly, the analysis yielded a thermal conductivity of 0.789 W/mK for glass beads which compares well (within 3%) to the 0.768 value reported by Raznjevic (15).

Table 2 lists the effective thermal diffusivities for silica gel, activated alumina, and activated carbon. Due to its low bulk density, the effective thermal diffusivity of the carbon-heptane system is higher than the others. Values found here of thermal conductivity compared well (within 5.5%) with those found in the literature (15), e.g., activated alumina was 0.641 W/mK versus 0.675 W/mK for pulverized aluminum oxide, and silica gel was 0.315 W/mK versus 0.326 W/mK for dry sand. It appears that, since close agreement was obtained between our experimentally determined thermal conductivities and those from the literature, the method adapted from Carslaw and Jaeger (11), Kunii and Smith (12), and Specchia et al. (13) is valid for this application.

Specific heats for silica, alumina, and carbon are nearly the same, and consequently, the ratios of solid/fluid heat capacities (assuming heptane

TABLE 2  
A Comparison of Thermal Properties for Silica Gel, Activated Alumina, and Activated Carbon

Adsorbent	Silica gel	Activated alumina	Activated carbon
$\rho_i$ (kg/m <sup>3</sup> )	2.1	3.2	1.7
$C_{p_s}$ (J/kgK)	920.0	837.0	1004.0
$\epsilon$	0.430	0.475	0.468
$\rho_{eff}$ (kg/m <sup>3</sup> )	1.14	1.38	0.97
$C_{p_{eff}}$ (J/kgK)	1841.0	1883.0	1923.0
$\alpha_{eff}$ (cm <sup>2</sup> /s)	$1.5 \times 10^{-3}$	$1.7 \times 10^{-3}$	$2.4 \times 10^{-3}$
$k_{eff}$ (W/mK)	0.315	0.442	0.448
$k_s$ (W/mK)	0.344	0.641	0.639
$\gamma = C_{p_s}/C_{p_f}$	0.41	0.37	0.44

as the fluid) are approximately equal. This ratio also happens to be the slope of the TSA operating line (for the traveling wave mode) on  $q_i$  versus  $c_i$  coordinates, which determines the final concentration following a thermal swing (16). Due to the low thermal-exchange capacity of alumina, the resulting high concentration product is less rich than that achieved with silica. Although carbon capacity for aromatics is almost as high as silica gel, the greater favorability associated with the isotherm results in lower separation factors compared to silica gel.

### E. Relationship between Dissipative Effects and Column Performance

In order to improve column performance in RTSA, it is important to maintain sharp thermal waves so that the adsorption front becomes as sharp as possible. Consequently, the effects of intraparticle mass diffusion and effective axial thermal dispersion upon temperature and concentration fronts must be understood. The Peclet numbers of both mass ( $vd_p/D_x$ ) and heat ( $vd_p/\alpha_x$ ) transfer and their relationship with the Reynolds number ( $\rho vd_p/\mu$ ) are at the center of this matter.

Gunn (17) presents the axial Peclet number for mass transfer versus Reynolds number for liquid and gas systems both experimentally and theoretically. For liquids having large Schmidt numbers, the Peclet number is nearly independent of the Reynolds number between Reynolds numbers of 0.01 and 10.0. In that range, the axial dispersion coefficient may be reduced by reducing particle size. Below and immediately above that range, however, a reduction in particle size does not proportionately reduce the effect of dispersive forces within the column, and concentration wave sharpness is only improved by intensification to a certain extent. Still, it is

imperative to use an adsorbent that exhibits fast adsorption and desorption kinetics.

On the other hand, the Prandtl number ( $C_p \mu / k_f$ ) for a fluid such as heptane is on the same order as that for gases. In fixed beds involving gases, the axial Peclet number for heat transfer does not reach an asymptotic value but rather varies linearly with the Reynolds number as shown by Gunn and DeSouza (18). Intensification does reduce the Peclet number further, but the effect upon thermal wave sharpness in RTSA is unnoticeable because the Peclet number is sufficiently low to minimize the effect of axial thermal dispersion. Accordingly, thermal conductivities of different adsorbents must be drastically different for one to be selected over the others, which is not the case for this application.

## V. CONCLUSIONS

Due to their dramatic effect on the feasibility of the process, the thermal-exchange capacity and particle size stand out as the most important adsorbent characteristics for a recycled temperature swing adsorption (RTSA) system. These control the size of the resulting equipment and the energy requirement because they dominate the extent of composition shifts that are possible, as well as the mass transfer rates and pressure drop. Other properties that affect performance in a secondary manner, i.e., by altering the shapes of the concentration or temperature waves, are interstitial and intraparticle porosities, particle density, solid heat capacity, effective (mass) diffusivity, and thermal diffusivity.

A specific application is discussed, viz., removing toluene and xylene from heptane. Silica gel was selected because it exhibited sufficient exchange capacity and was adequate with respect to the other criteria. Alumina and activated carbon were also investigated, but they were inappropriate for RTSA since their isotherm slopes did not vary with temperature at low concentrations. Molecular Sieve 13X and XAD-7 polymeric resin were insensitive to temperature at all concentrations.

The effective thermal diffusivity for silica gel (and heptane) was slightly lower than the other adsorbents, but the difference was not sufficient to alter by much the sharpness of temperature waves in the bed.

Finally, this separation application is being studied in bench-scale column experiments and will be the subject of a future report (6).

## NOTATION

$A_i$	Langmuir isotherm parameter
$B_i$	Langmuir isotherm parameter
$c_i$	concentration of Solute $i$ in solution

$C_p$	heat capacity
$d$	diameter
$D$	diffusivity
$D_z$	axial dispersion coefficient
$F$	fractional change
$Fo$	Fourier number
$J_0, J_1$	Bessel functions
$k_c$	film mass transfer coefficient
$k$	thermal conductivity
$l$	dimensionless length for conduction
$L$	column length
$M$	mass of adsorbent
$Nu$	Nusselt number
$\Delta P$	axial pressure drop
$Pe$	Peclet number
$Pr$	Prandtl number
$q_i$	quantity of Solute $i$ adsorbed by adsorbent
$Re$	Reynolds number
$R$	radius
$Sc$	Schmidt number
$t$	time
$T$	temperature
$v$	superficial velocity
$V$	volume of solution

### **Greek Letters**

$\alpha$	thermal diffusivity
$\beta$	mass balance parameter for transient uptake analysis
$\gamma$	heat capacity ratio of solid to fluid, $C_{p_s}/C_{p_f}$
$\epsilon$	effective void fraction of composite material
$\mu$	fluid viscosity
$\rho$	density
$\phi$	dimensionless film thickness

### **Subscripts**

$b$	bed
$bulk$	bulk phase
$c$	column
$eff$	effective
$f$	fluid
$p$	particle
$pore$	pore (fluid) phase

<i>s</i>	solid
<i>x</i>	axial
0	initial condition
$\infty$	final condition

### Acknowledgments

The authors are indebted to the companies that contributed the adsorbents used in this study, including Alcoa, Calgon, Davison, Rohm and Haas, and Union Carbide. Major funding for instruments was provided by a grant from Amoco Oil Company. The research was supported by grant CBT-86117680 from the National Science Foundation. In addition, the effort of Craig Barry and Suzanne Matz at The Ohio State University is appreciated.

### REFERENCES

1. N. H. Sweed, *AIChE Symp. Ser.*, 80(233), 44 (1984).
2. P. C. Wankat, *Large Scale Adsorption and Chromatography*, Vol. 1, CRC Press, Boca Raton, Florida, 1986.
3. R. D. Rieke, PhD Dissertation, University of California, Berkeley, 1973.
4. J. C. Kayser and K. S. Knaebel, in *Fundamentals of Adsorption* (A. I. Liapis, ed.), Engineering Foundation, New York, 1987.
5. K. S. Knaebel and R. L. Pigford, *Ind. Eng. Chem., Fundam.*, 22, 336-346 (1983).
6. M. J. Matz and K. S. Knaebel, *Ind. Eng. Chem., Res.*, Submitted.
7. E. J. Wilson and C. J. Geankoplis, *Ind. Eng. Chem., Fundam.*, 5, 9-14 (1966).
8. T. K. Sherwood, R. L. Pigford, and C. R. Wilke, *Mass Transfer*, McGraw-Hill, New York, 1975.
9. C. B. Barry, Private Communication, Ohio State University, 1989.
10. J. Crank, *Mathematics of Diffusion*, 2nd ed., Oxford University Press, London, 1975.
11. H. S. Carslaw and J. C. Jaeger, *Conduction of Heat in Solids*, Oxford University Press, London, 1959.
12. D. Kunii and J. M. Smith, *AIChE J.*, 6, 71-78 (1960).
13. U. Specchia, G. Baldi, and S. Sicardi, *Chem. Eng. Commun.*, 4, 361-380 (1980).
14. S. M. Matz, Private Communication, Ohio State University, 1989.
15. K. Raznjevic, *Handbook of Thermodynamics Tables and Charts*, McGraw-Hill, New York, 1976.
16. K. S. Knaebel, *AIChE Symp. Ser.*, 78, 128 (1982).
17. D. J. Gunn, *Chem. Eng. Sci.*, 42, 363-373 (1987).
18. D. J. Gunn and J. F. C. DeSouza, *Ibid.*, 29, 1363-1371 (1974).

Received by editor September 14, 1989

Revised February 25, 1990